Experimental Validation of the Pseudo-Rigid-Body Model of the MRI-Actuated Catheter

Tipakorn Greigarn, Russell Jackson, Taoming Liu, M. Cenk Çavuşoğlu

***Abstract*—An MRI-actuated catheter is a novel robotic catheter system that utilizes the MRI for both remote steering and visualization for catheter ablation of atrial fibrillation. Planning and control of the catheter requires a sufficiently fast yet accurate model of the catheter. The pseudo-rigid-body (PRB) model offers a reasonable trade-off between speed and accuracy by approximating the continuum catheter as rigid links connected by flexible joints, thus reducing the infinite degrees of freedom of the continuum mechanism to a finite one. In this paper, a PRB model of the MRI-actuated catheter is validated experimentally by comparing the deflections of the PRB model with the deflections of the catheter prototype.**

I. Introduction

Catheter ablation has become a standard treatment of atrial fibrillation [1]. An MRI-actuated catheter, proposed in [2], [3], is a novel robotic catheter concept that utilizes the MRI for visualization and remote steering. The current-carrying coils attached to the body of the catheter provide torques that remotely steer the catheter under the MRI's magnetic field. Precise control of the catheter is achieved by controlling the currents going through coils.

Planning and control of the MRI-actuated catheter requires a sufficiently fast and accurate model of the catheter. The pseudo-rigid-body (PRB) model has been used to model compliant mechanisms in various applications [4]. The PRB model is made of rigid links connected by flexible joints. The rigid links make it possible to apply robotic manipulation formulation to the model, while the flexible joints represents the elasticity of the continuum mechanism. The PRB model reduces the infinite degrees of freedom (DOFs) associated with a continuum mechanism down to a finite one.

While the accuracy of the PRB model increases with the number of joints [5], the higher DOFs also increase the computational cost associated with planning and control. In order to achieve a balanced trade-off between speed and accuracy, the parameters of the PRB model, namely link lengths and joint stiffnesses, have to be optimized, while the number of joints is held at a reasonable number.

This work was supported in part by the National Science Foundation under grants CISE IIS-1524363 and CISE IIS-1563805, and National Institutes of Health under grant R01 EB018108.

The authors are with the Department of Electrical Engineering and Computer Science, Case Western Reserve University, Cleveland, OH. They can be reached via email at txg92@case.edu, rcj33@case.edu, txl168@case.edu, and cavusoglu@case.edu respectively.

This paper presents experimental validation of the PRB model of a catheter prototype, as well as a parameter optimization of the PRB model. To validate the PRB model, the deflections of the PRB model with a different number of joints as well as a PRB model with optimal parameters are compared with the deflections of the catheter prototype.

The remainder of the paper is organized as follows. Related work is reviewed in Section II. The PRB model of the catheter is described in Section III. Experimental validation of the PRB model is presented in Section V. Conclusions are offered in Section VI.

II. Related Work

Continuum robots are widely used in medical applications because their flexible bodies are less harmful to the patients, and their hyper redundancy makes it possible to access hard-to-reach regions [6]. Several designs of continuum robot for different applications exist. For example, tendon-driven continuum manipulators are controlled by pulling tendons or cables routed through the conduits along the outer perimeter of the manipulators [7]. Concentric-tube robots are made of concentric pre-curved elastic tubes, which are controlled by sliding and rotating the tubes independently of one another [8]. The MRI-actuated catheters proposed in [2], [3] are steered by the torques from the Lorentz force between the MRI's static magnetic field and the magnetic moments generated from the current-carrying coils.

Continuum robots can be modeled in several ways. In the variable-curvature model, the position and the orientation of frames along the body of the continuum robot are expressed as a set of differential equations on the arc length of curve. The differential equations are solved as an initial value problem by numerical integration [9]. Another widely used model is the constant-curvature model [10]. In this model, the continuum robot is divided into segments, where each segment bends in a circular arc. A model of the MRI catheter based on the piecewise constant curvature assumption is presented in [11]. Another way of modeling a continuum robot is the PRB model, where the robot is divided into rigid links that are connected by flexible joints [4].

A PRB model typically consists of rigid links joined by revolute joints, but in some applications, prismatic joints are also used [12]. The compliance of the continuum mechanism is represented by torsional springs attached to the joints. A PRB model with n revolute joints is called an nR PRB model [13].

A 1R PRB model subjected to end forces and end moments are introduced in [14] and [15]. A PRB model with one revolute joint and two linear springs subjected to end forces and moments is presented in [12]. A PRB model with n uniform spring stiffnesses and uniform link lengthes is presented in [5]. While the parameters of the model are not optimized, the paper shows that the deflections of the model converge to the true deflections as the number of segments is increases. A 2R PRB model subjected to end forces and moments in opposing directions is presented in [16]. The additional joint in the model accounts for the deflections caused by the opposing forces and moments. A 3R PRB model is introduced in [13]. End forces and moments are considered separately and the optimal parameters are the average between the two cases. Brute force optimization over a discretized parameter space is used. In [17], the parameters of a 3R PRB model are chosen to minimize the cumulative delfection error from pure forces and pure moments applied at the end of the mechanism. Particle Swarm is used to optimize the parameters over a continuous parameter space. An optimization framework for an nR PRB model is proposed in [18]. A 3R PRB model is used to model a flexible catheter in [19].

The aforementioned PRB models consider planar motion with loads and reference points located at the tip of the mechanism. The constraints on the positions are removed in [20], where the loads and the reference points can be defined anywhere along the body of an nR PRB model. This paper further generalizes the approach in [20] by addressing non-planar deflections of the model. The nR PRB model considered in this paper has 3 DOFs joints, where the additional joint DOF models the twisting motion of the joint. A mathematical model of the new PRB model and a new objective function for parameter optimization are presented in this paper. The proposed PRB model is validated with delfection data obtained from an experiment.

III. The Pseudo-Rigid-Body Model

The PRB model of the MRI-actuated catheter is presented in this section. Section III-A presents forward kinematics of the PRB model with 3-DOF joints. Section III-B presents the calculation of the manipulator Jacobian. Section III-C presents quasi-static motion model via potential energy minimization.

A. Forward Kinematics

The PRB model consists of $n+1$ rigid links joined by n spherical joints, as shown in Fig. 1. Each spherical joint has three DOFs, two bending DOFs plus one twisting DOF. The rotation of the ith joint is parameterized by three rotation angles as follows, $\theta_i = [\theta_{ix}\ \theta_{iy}\ \theta_{iz}]^T \in \mathbb{R}^3$. This parameterization is chosen to represent a spherical joint instead of three intersecting revolute joints so that no order of rotation is assumed. Let the magnitude and the direction of rotation of the ith joint be denoted by $\phi_i = \|\theta_i\|$ and $\omega_i = \theta_i/\|\theta_i\|$, respectively, and let p_i denotes the initial position of the ith joint. The twist, $\hat{\xi}_i \in se(3)$, of the ith joint can be calculated as follows [21],

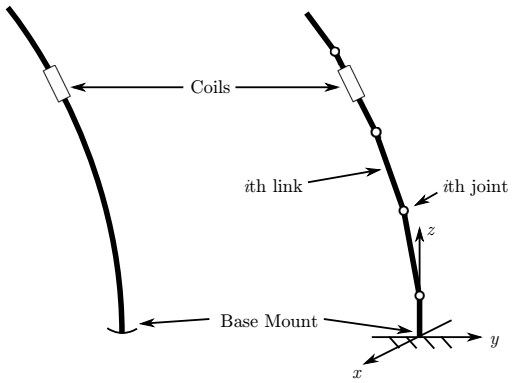

Fig. 1: The MRI-actuated catheter and the corresponding PRB model

$$\hat{\xi}_i = \begin{bmatrix} \hat{\omega}_i & -\omega_i \times p_i \\ 0 & 0 \end{bmatrix}, \tag{1}$$

where $\hat{\omega}_i \in so(3)$ is the skew-symmetric matrix counterpart of ω_i.

The shape of the PRB model of the catheter with n spherical joints is completely described by the joint angle vector $\theta = [\theta_1^T\ \theta_2^T\ \cdots\ \theta_n^T]^T \in \mathbb{R}^{3n}$. The configuration of a coordinate frame A attached to the jth link given joint angles θ is calculated from the product of exponentials formula as follows,

$$g_{sa}(\theta) = e^{\hat{\xi}_1\phi_1} e^{\hat{\xi}_2\phi_2} \cdots e^{\hat{\xi}_j\phi_j} g_{sa}(0), \tag{2}$$

where $g_{sa}(0)$ is the configuration of the frame A when $\theta = 0$, i.e., when the catheter is perfectly straight.

B. Manipulator Jacobian

Actuation and external forces interact with the catheter through the manipulator Jacobian. The manipulator Jacobian at A is calculated as follows,

$$J^b_{sa}(\theta) = \begin{bmatrix} \xi^\dagger_{1x} & \xi^\dagger_{1y} & \xi^\dagger_{1z} \cdots & \xi^\dagger_{jx} & \xi^\dagger_{jy} & \xi^\dagger_{jz} & 0 \cdots 0 \end{bmatrix}, \tag{3}$$

where the columns associated with the ith joint are calculated using the adjoint transformation as follows,

$$\xi^\dagger_{ix} = \mathrm{Ad}^{-1}_{(e^{\hat{\xi}_i\phi_i}\cdots e^{\hat{\xi}_n\phi_n} g_{sa}(0))} \xi_{ix}(\theta_i), \tag{4a}$$

$$\xi^\dagger_{iy} = \mathrm{Ad}^{-1}_{(e^{\hat{\xi}_i\phi_i}\cdots e^{\hat{\xi}_n\phi_n} g_{sa}(0))} \xi_{iy}(\theta_i), \tag{4b}$$

$$\xi^\dagger_{iz} = \mathrm{Ad}^{-1}_{(e^{\hat{\xi}_i\phi_i}\cdots e^{\hat{\xi}_n\phi_n} g_{sa}(0))} \xi_{iz}(\theta_i). \tag{4c}$$

For a spherical wrist implemented as three intersecting revolute joints, the columns of the Jacobian are the twists written with respect to the body frame. For the parameterization of the spherical joints of the PRB model in this paper, the twists, $\xi^\dagger_{ix}$, $\xi^\dagger_{iy}$, and $\xi^\dagger_{iz}$, in (3) are not only written with respect to the body frame, but the twists of the ith joint, $\xi_{ix}(\theta_i)$, $\xi_{iy}(\theta_i)$, and $\xi_{iz}(\theta_i)$, are also functions of θ_{ix}, θ_{iy}, and θ_{iz}. Suppose the rotation matrix associated with the ith joint is $R(\theta_i) = e^{\hat{\omega}_i\phi_i}$.

The bases of the instantaneous angular velocity of the i joint are given by,

$$\hat{\omega}_{ix}(\theta_i) = \frac{\partial R(\theta_i)}{\partial \theta_{ix}} R^T(\theta_i), \tag{5a}$$

$$\hat{\omega}_{iy}(\theta_i) = \frac{\partial R(\theta_i)}{\partial \theta_{iy}} R^T(\theta_i), \tag{5b}$$

$$\hat{\omega}_{iz}(\theta_i) = \frac{\partial R(\theta_i)}{\partial \theta_{iz}} R^T(\theta_i). \tag{5c}$$

Let $\omega_{ix}(\theta_i), \omega_{iy}(\theta_i), \omega_{iz}(\theta_i) \in \mathbb{R}^3$ denote the vector representations of $\hat{\omega}_{ix}(\theta_i), \hat{\omega}_{iy}(\theta_i), \hat{\omega}_{iz}(\theta_i) \in so(3)$. The twists in (4) are written in terms of the three vectors as follows,

$$\xi_{ix}(\theta_i) = \begin{bmatrix} -\omega_{ix}(\theta_i) \times p_i, \\ \omega_{ix}(\theta_i) \end{bmatrix} \tag{6a}$$

$$\xi_{iy}(\theta_i) = \begin{bmatrix} -\omega_{iy}(\theta_i) \times p_i, \\ \omega_{iy}(\theta_i) \end{bmatrix} \tag{6b}$$

$$\xi_{iz}(\theta_i) = \begin{bmatrix} -\omega_{iz}(\theta_i) \times p_i, \\ \omega_{iz}(\theta_i) \end{bmatrix} \tag{6c}$$

where p_i is the position of the ith joint.

Suppose there is an external wrench $F \in \mathbb{R}^6$ applied at the frame A on the jth link of the catheter. The joint torques, denoted by τ, produced by F at A is simply

$$\tau = (J^b_{sa})^T F. \tag{7}$$

C. Quasi-Static Motion Model

Since the catheter is designed to operate at a speed much lower than its bandwidth, the quasi-static assumption is used to calculate the motion model, i.e., the shape of the catheter given the currents. The quasi-static configuration of the catheter given external forces and actuation currents is calculated by minimizing the potential energy of the catheter,

$$\min_{\theta} \ \frac{1}{2}\theta^T K \theta - \sum_{i=1}^{m} B_0^T \mu_i(\theta, u_i) + \sum_{j=1}^{n} (v_j(\theta) - w_j(\theta, F_j)). \tag{8}$$

The first term in the objective function is the potential energy due to the internal stiffness of the catheter, where K is the stiffness matrix. The second term is the summation of the potential energy of the magnetic moments from the actuators [22], where B_0 is the MRI's magnetic field vector, μ_i is the magnetic moment of the ith actuator expressed in the MRI frame, and u_i is the actuation, i.e., the currents sent to the ith coil set. The last term is the sum of the potential energy due to gravity, v_j, minus the work, w_j, done by the applied wrench, F_j, on the jth link.

IV. Parameter Optimization

To achieve a good trade-off between speed and accuracy, the parameters of the PRB model are optimized such that the deflections of the PRB model closely approximates those of the reference model. In this paper, the continuum model described in [11] is chosen as the reference model.

A. Optimization Problem

The parameters of the PRB model are optimized such that the deflections of the PRB model closely approximate those of the continuum model under the same set of loads. The parameter optimization problem is defined as follows,

$$\min_{r,k} \ \sum_{i=1}^{|\mathcal{P}|} \sum_{j=1}^{|\mathcal{F}|} \alpha_i \frac{\|x_{ij} - \bar{x}_{ij}\|}{r_{\text{total}}} + \beta_i \frac{\text{acos}(|q_{ij} \cdot \bar{q}_{ij}|)}{\pi}, \tag{9a}$$

$$\text{s.t.} \ \sum_{m=1}^{n} r_m = r_{\text{total}}, \tag{9b}$$

where r is a vector containing the link lengths, k is a vector containing the joint stiffnesses, $\mathcal{P}$ is a set of reference points, $\mathcal{F}$ is a set of loads, where each load is a set of wrenches acting on multiple points on the body of the catheter. The position and the orientation of the ith reference point due to the jth load on the PRB and the continuum models are denoted by (x_{ij}, q_{ij}) and $(\bar{x}_{ij}, \bar{q}_{ij})$, respectively. The weights, α_i and βi, specify the relative degree of importance of the position and the orientation at the ith reference point. The objective function (9a) is a weighted sum of position and orientation errors from all the reference points due to all the loads. The orientation error term in the objective function is a distance metric in $SO(3)$. Arccosine of the inner product of the quaternion is chosen as the distance metric between two elements of $SO(3)$ [23]. The constraint (9b) ensures that the sum of the length of the links is equal to the total length of the catheter.

The parameter optimization problem (9) is solved in the following manner. Before the optimization algorithm starts, the deflections of the continuum model subjected to the loads in $\mathcal{F}$ are calculated. This only has to be calculated once since it is independent of the parameters of the PRB model. During each optimization iteration, the deflections of the PRB model subjected to the same loads in $\mathcal{F}$ are calculated from the quasi-static motion model described in (8). The deflections of the two models are compared, and the optimization algorithm adjusts the link lengths and the joint stiffnesses. Since the optimization problem is non-convex, Particle Swarm Optimization, which is a global optimization algorithm, is chosen as the solver.

B. Optimization Results

Since the catheter has one coil set, a PRB model with three joints is chosen as the base-line model. The first two joints from the base of the catheter give the PRB model enough DOFs to deflect when the coils are energized. The last joint represents the compliance of the catheter when it is in contact with a surface. Following the notation mentioned in Section II, the three-joint model will be referred to as the 3R model. As the base-line model, the 3R model has uniform link lengths, and the joint stiffnesses are calculated from the mechanical properties of the material.

The loads used to optimize the parameter of the PRB model are listed in Table I. The forces and torques in Table I are components of wrenches of the form $F = [f_x \ f_y \ f_z \ \tau_x \ \tau_y \ \tau_z]^T \in$

TABLE I: External loads used to optimize the parameters. Forces are in N and torques are in N·mm. Five linearly spaced points between min and max are used in the optimization.

	Coils			End-Effector		
	f_x	τ_x	τ_z	f_x	f_z	τ_z
Min	0.01	0.01	0.001	0.001	0.001	0.01
Max	0.50	0.20	0.020	0.020	0.005	0.20

TABLE II: PRB optimal parameters

Parameter	Value
r (mm)	$[12.78, 57.55, 30.79, 0.23]$
k (rad/Nmm)	$[0.5441, 0.3836, 0.4158, 0.8039, 4.5943, 7.9468]$

$\mathbb{R}^6$. The frame of reference of the catheter is centered at the base mount. The z-axis points along the length of the catheter, while the y-axis is aligned with the magnetic field of the MRI. The torques, τ_x and τ_z, at the coil set represent bending torques from the magnetic moment, while the force f_x represents perturbations on the catheter. At the end-effector, the force f_x represents perturbation forces, while f_z represents contact forces. The torque τ_z excites torsional rotations of the last joint. To separate the effects of the forces and torques applied to the catheter, each force/torque is applied separately except for the compressive force at the end-effector, f_z, which is applied with an equal amount of bending force, f_x, to eliminate buckling.

The parameters obtained from the optimization problem are listed in Table II. Let the PRB model with the optimal parameters be denoted by 3R* model (* for the optimal parameters). The end-effector positions of the 3R and the 3R* catheter along a circular trajectory are compared with those of the continuum model in Fig. 2. The currents that drive the catheter are generated from the continuum model [11]. The errors between the end-effector positions of the 3R and the 3R* models when compared to the continuum model are plotted in Fig. 3. Note that the error of the 3R* model is lower than the 3R model for the majority of the trajectory.

V. Experimental Validation

Experimental validation of the PRB model is presented in this section. The catheter prototype used in the experiment is described in Section V-A. The experimental setup is explained in Section V-B. The deflections of the PRB model are compared with the deflections of the catheter prototype in Section V-C.

A. Catheter Prototype

The catheter prototype has one coil set with three mutually orthogonal coils. The axial coil has 100 turns while the two side coils each have 30 turns. The coils are made of 38-guage solid core enameled copper wire. The catheter is made of a silicone tube with the outer diameter of 3.18 mm and the length of 101.35 mm (Part number: T2011, QOSINA, Edgewood, NY). The rest of the parameters are listed in Table III.

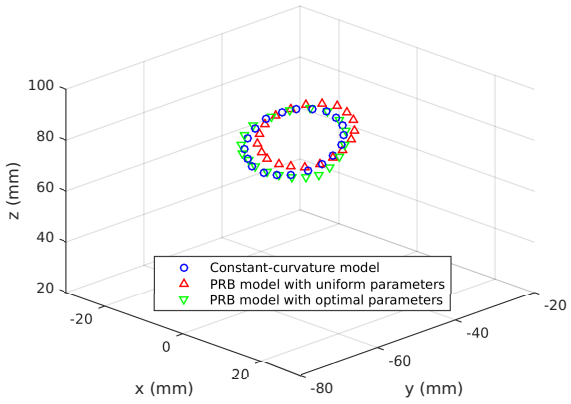

Fig. 2: End-effector positions of the continuum, the 3R PRB, and the 3R* PRB model, following a circular trajectory.

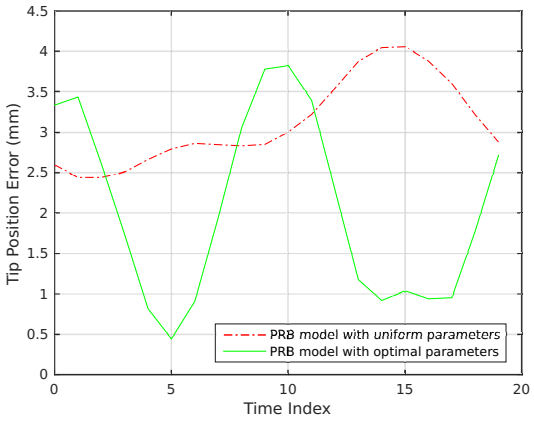

Fig. 3: End-effector position errors of the 3R and the 3R* models when compared with the continuum model.

TABLE III: Catheter parameters

Parameter	Value
Young's modulus	5.05 MPa
Shear modulus	1.87 Unit
Inner diameter	1.98 mm
Outer diameter	3.18 mm
Total length	101.35 mm
Distance of coil set from base	72.9 mm
Axial coil winding turns	100
Side coil winding turns	30
Axial coil surface area	15.55 mm^2
Side coil surface area	48.02 mm^2

B. Experimental Setup

The experiment is conducted in inside a 3 T clinical MRI scanner (Skyra, Siemens Medical Solutions, Erlangen, Germany). The catheter is mounted vertically on the top of an

aquarium tank filled with water. The setup is then placed at the isocenter of the scanner during the experiment.

The three-dimensional shape of the catheter is determined from stereo images. For safety reasons, the camera has to stay at least 6 m away from the isocenter of the scanner. As a result, depth perception is not possible via stereo cameras. To circumvent the problem, a mirror is placed at a 45 degrees angle next to the catheter to provide a side view of the catheter. A single camera records images of the catheter and its reflection in the mirror. The two images are combined to construct the 3D shape of the catheter. This imaging system is known as a catadioptric stereo system [24].

C. Results

The defections of four PRB models are compared with the deflections of the catheter prototype in this section. To show that the deflections of the PRB model converge to those of the continuum robot as the number of joints increases, three PRB models with three, six, and nine joints, as well as the model with the optimal parameters from Section IV, are studied. They are referred to as the 3R, 6R, 9R, and 3R* model, respectively. The first three PRB models have uniform link lengths, and their joint stiffnesses are calculated from the parameters of the prototype listed in Table III.

Fig. 4 shows the distance between the PRB models' and the prototype's end-effector positions when the currents shown in Fig. 5 are applied to the catheter. Note that the position error decreases monotonically for the 3R, 6R, and 9R catheter in Fig. 4. The 3R* PRB model seems to have the opposite error profile when compared to the other three, i.e., the 3R* model achieves its lowest error while the others are at their highest and vice versa. The shape of the PRB models at time index 5 and 11 are shown in Fig. 6. The deflections from these two time indices are shown because they are right around the point when the 3R* PRB model is at its lowest and highest errors, respectively. The average computational time of the inverse kinematics of the 3R, 6R, 9R, and 3R* PRB models are 0.2093 s, 0.5761 s, 1.1957 s, 0.2500 s, respectively. The PRB models are implemented in MATLAB R2015a running on an Ubuntu machine with Intel Core-i5 3.10 GHz processor and 8 GB memory.

VI. Conclusions

In this paper, a mathematical model of the PRB model with 3-DOF joints is presented, and a formulation for optimizing the parameters of the PRB model is proposed. The PRB model is validated by comparing the deflections of the PRB model with those of the catheter prototype under the same set of actuations. The results show that the end-effector position error decreases monotonically when the number of joints of the model increases. On average, the 3-joint PRB model with optimal parameters has higher accuracy than the 3-joint PRB model with uniform parameters.

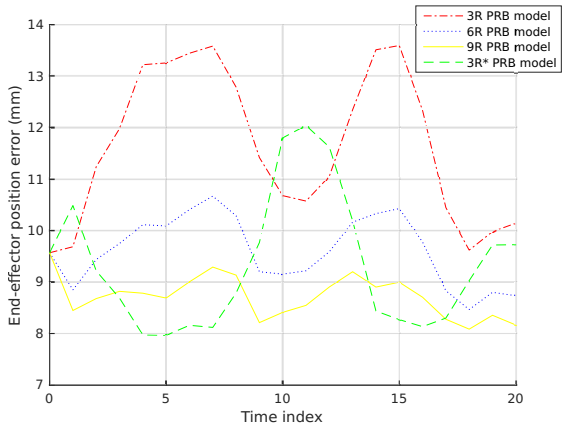

Fig. 4: Tip position error of the PRB models when compared with the catheter prototype.

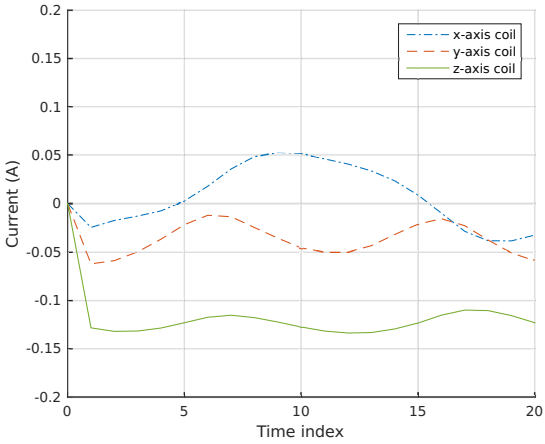

Fig. 5: Current trajectories used in the experiment.

References

[1] H. Calkins *et al.*, "2012 HRS/EHRA/ECAS Expert Consensus Statement on Catheter and Surgical Ablation of Atrial Fibrillation: Recommendations for Patient Selection, Procedural Techniques, Patient Management and Follow-up, Definitions, Endpoints, and Research Trial Design," *Europace*, vol. 14, no. 4, pp. 528–606, apr 2012.

[2] T. P. L. Roberts, W. V. Hassenzahl, S. W. Hetts, and R. L. Arenson, "Remote control of catheter tip deflection: An opportunity for interventional MRI," *Magnetic Resonance in Medicine*, vol. 48, no. 6, pp. 1091–1095, dec 2002.

[3] N. Gudino, J. A. Heilman, J. J. Derakhshan, J. L. Sunshine, J. L. Duerk, and M. A. Griswold, "Control of intravascular catheters using an array of active steering coils," *Medical Physics*, vol. 38, no. 7, pp. 4215–4224, 2011.

[4] L. L. Howell, S. P. Magleby, and B. M. Olsen, *Handbook of compliant mechanisms*. Wiley Online Library, 2013.

[5] L. Saggere and S. Kota, "Synthesis of Planar, Compliant Four-Bar Mechanisms for Compliant-Segment Motion Generation," *Journal of Mechanical Design*, vol. 123, p. 535, 2001.

[6] J. Burgner-Kahrs, D. C. Rucker, and H. Choset, "Continuum robots for medical applications: A survey," *IEEE Transactions on Robotics*, vol. 31, no. 6, pp. 1261–1280, 2015.

[7] D. B. Camarillo, C. F. Milne, C. R. Carlson, M. R. Zinn, and J. K. Salisbury, "Mechanics modeling of tendon-driven continuum manipulators," *IEEE Transactions on Robotics*, vol. 24, no. 6, pp. 1262–1273, 2008.

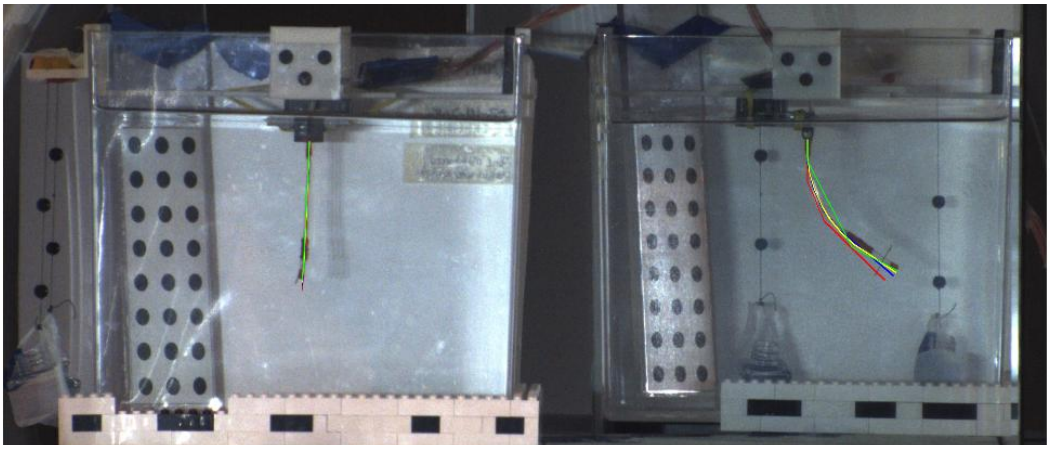

(a) Time index = 5

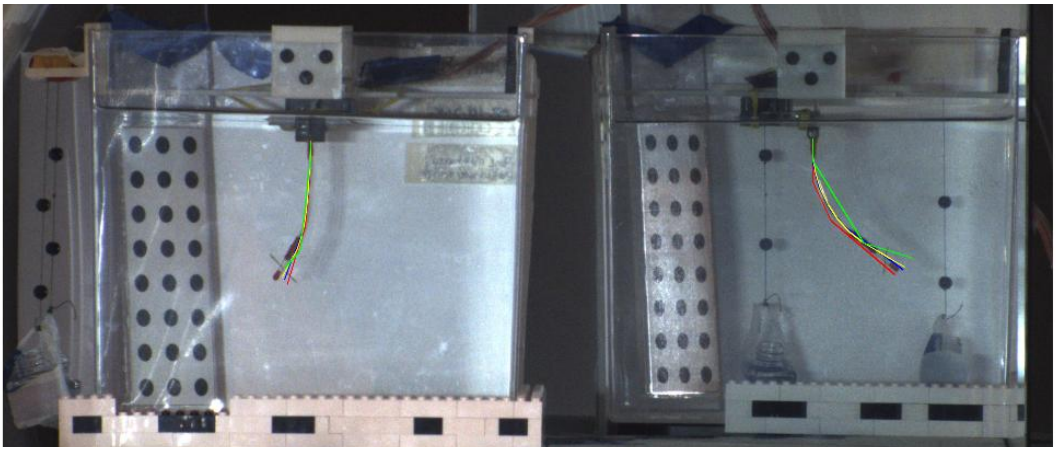

(b) Time index = 11

Fig. 6: Deflections of the PRB models are plotted on the raw images from the experiment. The image of the actual catheter is on the left side, while the image of the catheter reflected from the mirror is on the right side. The 3R, 6R, 9R, and 3R* PRB models are shown in red, blue, yellow, and green, respectively. The direction of the magnetic field goes into the page.

[8] P. E. Dupont, J. Lock, B. Itkowitz, and E. Butler, "Design and control of concentric-tube robots," *IEEE Transactions on Robotics*, vol. 26, no. 2, pp. 209–225, 2010.

[9] G. S. Chirikjian and J. W. Burdick, "The kinematics of hyper-redundant robot locomotion," *IEEE transactions on robotics and automation*, vol. 11, no. 6, pp. 781–793, 1995.

[10] R. J. Webster and B. A. Jones, "Design and kinematic modeling of constant curvature continuum robots: A review," *The International Journal of Robotics Research*, 2010.

[11] T. Liu, N. Lombard Poirot, D. Franson, N. Seiberlich, M. Griswold, and M. Cavusoglu, "Modeling and Validation of the Three Dimensional Deflection of an MRI-Compatible Magnetically-Actuated Steerable Catheter," *IEEE Transactions on Biomedical Engineering*, 2015.

[12] A. Saxena and S. N. Kramer, "A Simple and Accurate Method for Determining Large Deflections in Compliant Mechanisms Subjected to End Forces and Moments," *Journal of Mechanical Design*, vol. 120, p. 392, 1998.

[13] H.-J. Su, "A Pseudorigid-Body 3R Model for Determining Large Deflection of Cantilever Beams Subject to Tip Loads," *Journal of Mechanisms and Robotics*, vol. 1, no. 2, 2009.

[14] L. L. Howell and A. Midha, "Parametric deflection approximations for end-loaded, large-deflection beams in compliant mechanisms," *Journal of Mechanical Design*, vol. 117, no. 1, pp. 156–165, 1995.

[15] L. L. Howell, "The design and analysis of large-deflection members in compliant mechanisms," Ph.D. dissertation, 1991.

[16] C. Kimball and L.-W. Tsai, "Modeling of Flexural Beams Subjected to Arbitrary End Loads," *Journal of Mechanical Design*, vol. 124, p. 223, 2002.

[17] G. Chen, B. Xiong, and X. Huang, "Finding the optimal characteristic parameters for 3R pseudo-rigid-body model using an improved particle swarm optimizer," *Precision Engineering*, vol. 35, pp. 505–511, 2011.

[18] V. K. Venkiteswaran and H.-J. Su, "A parameter optimization framework for determining the pseudo-rigid-body model of cantilever-beams," *Precision Engineering*, 2014.

[19] M. Khoshnam and R. V. Patel, "A pseudo-rigid-body 3R model for a steerable ablation catheter," in *Robotics and Automation (ICRA), 2013 IEEE International Conference on*. IEEE, may 2013, pp. 4427–4432.

[20] T. Greigarn and M. C. Cavusoglu, "Pseudo-Rigid-Body Model and Kinematic Analysis of MRI-Actuated Catheters," in *Robotics and Automation (ICRA), 2015 IEEE International Conference on*, 2015.

[21] R. M. Murray, Z. Li, S. S. Sastry, and S. S. Sastry, *A Mathematical Introduction to Robotic Manipulation*, 1st ed. CRC Press, mar 1994.

[22] D. Dugdale and D. E. Dugdale, *Essentials of electromagnetism*. Springer Science & Business Media, 1993.

[23] D. Q. Huynh, "Metrics for 3d rotations: Comparison and analysis," *Journal of Mathematical Imaging and Vision*, vol. 35, no. 2, pp. 155–164, 2009.

[24] R. C. Jackson, T. Liu, and M. C. avuolu, "Catadioptric stereo tracking for three dimensional shape measurement of mri guided catheters," in *2016 IEEE International Conference on Robotics and Automation (ICRA)*, May 2016, pp. 4422–4428.